

# Osteogenic activity of MG63 cells on bone-like hydroxyapatite/collagen nanocomposite sponges

Teruaki Yoshida · Masanori Kikuchi ·  
Yoshihisa Koyama · Kazuo Takakuda

Received: 6 August 2009 / Accepted: 6 November 2009 / Published online: 19 November 2009  
© Springer Science+Business Media, LLC 2009

**Abstract** The hydroxyapatite/collagen (HAp/Col) sponge with 95% (v/v) porosity was prepared by freeze-drying of a HAp/Col fiber suspension. MG63 cells were seeded onto the HAp/Col sponge and cultured under a pressure/perfusion condition with osteogenic supplements. A collagen (Col) sponge was used as a control. The cells with sponge were examined by a histology, total DNA content and gene expression. The cells showed good attachment and proliferation everywhere in the HAp/Col sponge, while the cells mainly proliferated at the peripheral part of the Col sponge. Thus, total DNA content in the HAp/Col sponges reached 1.8 times greater than that in the Col sponges at Day 21. Further, the cells and extracellular matrix only in the HAp/Col sponge were calcified, although the cells in both sponge evenly expressed osteogenic gene. These results suggest that the HAp/Col sponge could be useful as a scaffold for bone tissue engineering.

## 1 Introduction

The transplantation of autologous bone for repairing bone defects is limited by the shortage of available bones and by the morbidity of donor sites. Allogenic and xenogenic transplantations often cause undesired immunological rejection from the recipient. Because of the numerous

complications associated with these tissue-based materials, synthetic bone void fillers are being developed as alternatives of the tissue-based materials [1]. With the recent advances in tissue engineering, many kinds of materials have been tried as bone tissue engineering scaffolds. Orthopedic and dental fields require a biodegradable and biomimetic material that can induce and promote new bone formation by osteogenic cells at a required site in a reasonable period. Ideally, such material would be three-dimensional (3D) and have an appropriate porosity with an interconnected porous structure to support cell proliferation and ingrowth. Hydroxyapatite (HAp) is the main inorganic component of bone and is recognized as a good bone filler material, because of its osteoconductivity. Due to its difference of mechanical and biochemical properties from those of natural bone, however, HAp-based materials, when transplanted, remain in the bone for the patients' lifetime and induce fracture at or around the site of transplantation. Various biocompatible polymers (e.g., poly-L-lactide (PLA), polyglycolide (PGA), poly-L-lactide-*co*-glycolide (PLGA) and collagen) and HAp/biocompatible polymer composites have also been studied for bone tissue engineering application [2–12]. However, the degradation products of these synthetic polymers reduce the local pH, accelerating polymer degradation and potentially induce inflammatory responses [13]. Even for HAp/biocompatible polymer composites, their degradation process is far different from the resorption process of autologous bone. Composites of HAp and collagen, the main organic component of bone, are expected to be promising as bone substitutes; thus, many types of composites have been proposed [14–18]. The key to successful bone regeneration is to provide sufficient osteogenic progenitor cells in a suitable delivery vehicle to ensure osteoblastic differentiation and optimal secretory activity at the site of bone defect. Du et al.

---

T. Yoshida · Y. Koyama · K. Takakuda  
Institute of Biomaterials and Bioengineering, Tokyo Medical and Dental University, 2-3-10Kanda-Surugadai, Chiyoda-ku, Tokyo 101-0062, Japan

T. Yoshida · M. Kikuchi (✉)  
Biomaterials Center, National Institute for Materials Science, 1-1 Namiki, Tsukuba, Ibaraki 305-0044, Japan  
e-mail: KIKUCHI.Masanori@nims.go.jp

have developed a biomimetic nano-HA/collagen (nHAC) scaffold and confirmed that nHAC conjugated with bone particles show good osteointegration [16]. Wu et al. have prepared a reconstituted fibrous collagen microsphere in which hydroxyapatite particles are dispersed and shown that osteoblasts are capable of proliferation, differentiation and mineralization in the matrix of the microspheres [17]. Other methods to improve the biomimetic qualities of biomaterials are also available. Porous biomimetic matrices may provide a suitable microenvironment that promotes osteoblast proliferation and osteogenesis. Previously, we developed a self-organized, bone-like HAp/collagen (HAp/Col) nanocomposite as an artificial bone material and reported good biological reaction in vivo [19]. Furthermore, we also developed a sponge-like 3D porous body of the HAp/Col nanocomposite [20]. However, we have not evaluated viability and osteogenic activity of cells in this material in vitro so far. For proliferation of cells in 3D scaffolds, one of the most important aspects is to maintain cells' viability and functions during proliferation in vitro by applying nutrition, organic supplements, and mechanical stimuli. Cartmell reported that culture medium perfusion through three-dimensional (3D) porous cellular constructs was useful to maintain cell viability and function [21]. Glowacki and Mueller reported that medium perfusion at low flow rates (1.3 ml/min) maintains the viability and function of murine bone marrow [22] and osteosarcoma cells [23] cultured in 3D collagen sponges. On the basis of these data, Mizuno et al. developed a novel pressure/perfusion culture system to apply a hydrostatic fluid pressure (HFP) and medium perfusion to chondroblasts cultured in the sponge to maintain the chondrogenic activity of the cells [24]. We also found that this pressure/perfusion system enhances the osteogenic activity of osteoblastic MG63 cells as well as their viability in the center of collagen sponges [25], which is generally considered as one of the most promising tissue engineering scaffolds. In this study, a highly porous, 3D HAp/Col nanocomposite sponge was prepared, and proliferation and osteogenic response of human osteoblast-like cells, MG63, on/in the HAp/Col sponge were investigated using pressure/perfusion culture system to evaluate the HAp/Col sponge as a bone tissue engineering scaffold. A collagen sponge as an excellent tissue engineering scaffold was used as a control [26].

## 2 Materials and method

### 2.1 Preparation of HAp/Col nanocomposite sponge

HAp/Col sponges were prepared from HAp/Col nanocomposite fibers. The HAp/Col nanocomposite fibers were synthesized by the simultaneous titration coprecipitation

method described in Ref. [19] with slight modification that the HAp/Col mass ratio was changed into 70/30 instead of the previous 80/20 to approximate mass ratio of the natural bone. Briefly,  $\text{Ca}(\text{OH})_2$ , obtained by decarbonation and hydration of  $\text{CaCO}_3$  (alkaline analysis grade; Wako Pure Chemical Industries, Osaka, Japan),  $\text{H}_3\text{PO}_4$  (regent grade; Wako Pure Chemical Industries) and type-I collagen (atelocollagen extracted from porcine dermis, biomaterial grade; Nitta Gelatin, Osaka, Japan) were used as starting materials. Two-hundred millimolars of  $\text{Ca}(\text{OH})_2$  aqueous suspension and 60 mM of  $\text{H}_3\text{PO}_4$  aqueous solution containing collagen were simultaneously added into 400 ml of distilled water in a reaction vessel through tube pumps. The amounts of the starting materials,  $\text{Ca}(\text{OH})_2$ ,  $\text{H}_3\text{PO}_4$  and collagen, were calculated based on a rational calculation according to the ref. 19 in which the synthesis reaction almost occurred ideally. For instance, to obtain 10 g of HAp/Col with HAp/Col mass ratio of 70/30, 348.4 ml of 200 mM  $\text{Ca}(\text{OH})_2$  suspension, 696.8 ml of 60 mM  $\text{H}_3\text{PO}_4$  solution containing 3 g of collagen were used for synthesis. The pH of reaction solution was maintained at 9 by a pH controller connected to the tube pumps, and the temperature was controlled at 40°C with a water bath as schematically illustrated in Fig. 1. The HAp/Col nanocomposite fibers obtained were filtered and freeze-dried at  $-20^\circ\text{C}$ . A weight ratio of the freeze-dried composite was quantified by differential thermal analysis using a thermogravimetry (TG-DTA) (Thermo Plus TG8120; Rigaku, Tokyo, Japan) at temperature ranging from room temperature to 1200°C with a heating rate of 20°C/min. The HAp/Col sponges were prepared by freeze-dry removal of ice crystals according to the previous method [20] with a slight modification. Briefly,

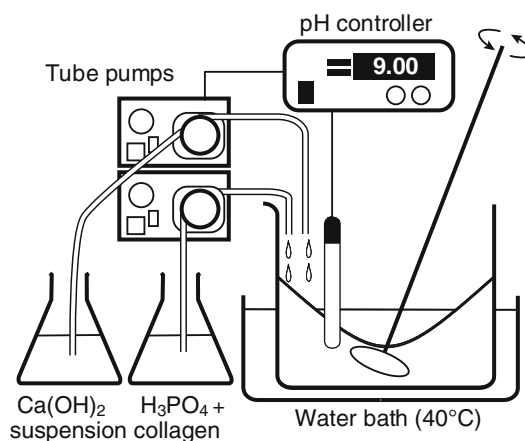


**Fig. 1** HAp/Col nanocomposite synthesis device. The composites were synthesized by a simultaneous titration coprecipitation method. The pH of the reaction solution was maintained at 9 by the autotitration unit equipped with a pH controller, and the temperature of the reaction solution was controlled at 40°C by water bath

the HAp/Col nanocomposite fibers were mixed with Dulbecco's phosphate buffered saline (PBS). Supplemental collagen suspension, which was added to maintain homogeneous dispersion HAp/Col fiber in the previous method, was not added to the mixture in this study due to prevent covering the HAp/Col surface with pure collagen. The mixing ratio of PBS and the HAp/Col fibers was regulated that the final porosities of the sponge to be 95% (v/v), e.g., 95 ml of PBS and 10.6 g of the HAp/Col were mixed to prepare 100 cm<sup>3</sup> of the HAp/Col sponge. The HAp/Col mixture was incubated at 37°C for 1 h and frozen at −20°C. The frozen mixture was freeze-dried at −20°C and cross-linked by vacuum heating at 140°C for 12 h. The HAp/Col sponges obtained were cut into test pieces ( $\phi$  8 mm  $\times$  5 mm in size).

The porosity of the HAp/Col sponges was calculated from the measured weight and measured volume of the test piece, where the theoretical density of the HAp/Col composite was 2.12 g/cm<sup>3</sup>. Finally, the sponges were sterilized by ethylene oxide gas. A collagen sponge was used as a control and prepared at the same size as the HAp/Col sponge by the following procedures. The type-I atelocollagen dispersed in PBS was poured into a mold made of Tygon<sup>®</sup> tubing, incubated at 37°C for 1 h, frozen at −20°C, freeze-dried and cross-linked by vacuum heating at 140°C for 12 h. The microstructures of HAp/Col and Col sponges were observed scanning electron microscopy (SEM) (JSM-5600LV; JEOL, Tokyo, Japan). Mean pore size of these sponges was calculated from approximately 50 pore diameters measured from SEM photographs. Mean wall thickness of these sponges was also calculated from approximately 50 wall thicknesses measured from SEM photographs.

Both HAp/Col and Col sponges obtained were incubated for 5 days in growth medium (Dulbecco's modified Eagle's medium; Sigma-Aldrich, St. Louis, MO, USA) supplemented with 10% (v/v) fetal bovine serum (Invitrogen, Carlsbad, CA, USA), 100 U/ml penicillin and 100  $\mu$ g/ml streptomycin (Invitrogen) to allow saturation of ion adsorptions on the sponges according to the preliminary examined adsorption isotherms of Ca and Mg ions onto the HAp/Col sponge.

## 2.2 Cell seeding and culture conditions

A pressure/perfusion culture system was designed according to the previous report [24]. This system applies HFP to the sponges with constant perfusion of a medium. The medium in the reservoir was sent through a debubbler, perfusion pump, pressure gauge, glass-column and back-pressure regulator and returned to the reservoir (Fig. 2). The flow rate was controlled by the perfusion pump, and constant HFP was applied by the back pressure regulator.

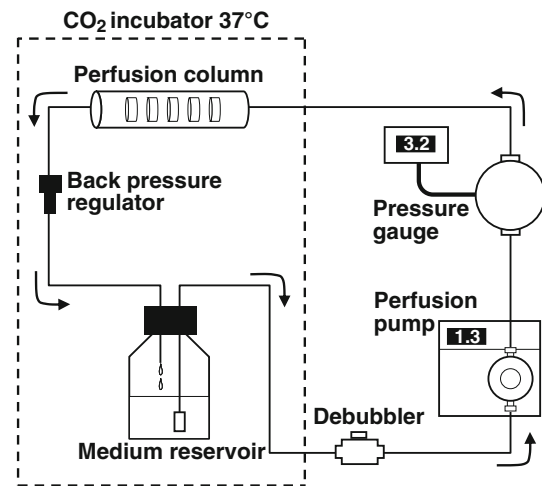


**Fig. 2** Pressure/perfusion culture system. The 3D culture unit was designed for application of pressure to the sponges with constant perfusion of the medium

All components of the apparatus except for the debubbler, pump and pressure gauge were maintained within a 5% CO<sub>2</sub> incubator. The tubing was introduced into the incubator just behind the pressure gauge. The length of tubing to the column inlet placed in the incubator was approximately 15 m to allow increasing the medium temperature to 37°C, because the medium temperature was drop down to room temperature passing through the debubbler, perfusion pump and pressure gauge.

The human osteoblast-like cell line, MG63, derived from human osteosarcoma was used for the experiment. MG63 cells were cultured in growth medium at 37°C in a humidified 5% CO<sub>2</sub> atmosphere. The cells were harvested and suspended at a concentration of  $2 \times 10^7$  cells/ml. Each sponge set into a hand-made seeding device to prevent cell effusion from the sponge during seeding was placed into a well of 6-well tissue culture plates (Falcon<sup>®</sup>; Becton, Dickinson and Co., Franklin Lakes, NJ, USA). A 50- $\mu$ l cell suspension containing  $1 \times 10^6$  cells was seeded onto each sponge and incubated for 1 h to allow initial cell attachment to the sponges. Then, 5 ml of growth medium was added to each well, and the cells with sponge were cultured under static (conventional) condition for 24 h to complete cell attachment on the sponge. At 24 h after seeding, each of the sponges was removed from the device and transferred into a pressure/perfusion column. During the first 6 days, only perfusion was applied at 1.3 ml/min to the columns to support cell proliferation. At Day 7, the medium was changed to osteogenic medium that is composed of growth medium supplemented with 50  $\mu$ g/ml L-ascorbic acid phosphate magnesium salt (Wako Pure Chemicals Industries) and 10 mM  $\beta$ -glycerophosphate (Sigma-Aldrich Co., USA), and pressure (3.2 MPa) was applied together

with 1.3 ml/min perfusion. The medium was changed every 3 days (2.5 ml/sponge/day). Pressure/perfusion culture was continued up to 21 days.

### 2.3 Histological observation

The porous morphologies of the sponge and cell-sponge connection were studied by optical microscopy (BX51; OLYMPUS, Tokyo, Japan) and scanning electron microscopy (SEM) (JSM-5600LV; JEOL, Tokyo, Japan). Two sponges each were harvested at 1, 7, 10, 14 and 21 days, fixed with Bouin's fluid and dehydrated in a graded ethanol series. For optical microscopic observation, sponges were separately immersed in xylene and embedded in paraffin. Paraffin blocks were sectioned at 5  $\mu\text{m}$  and stained with hematoxylin and eosin (HE) for visualization of cell proliferation. Other sponges were separately soaked in t-butanol and vacuum dried at 0°C for SEM observation to investigate initial cell attachment and proliferation on/in the sponge. The SEM observation was operated at an accelerating voltage of 10 kV. Energy dispersive spectroscopy (EDS) was also used to investigate matrix mineralization.

### 2.4 Total DNA quantitative analysis

The DNA content of MG63 cells on/in the sponges was used as a measure of cell proliferation. After 3, 7, 10, 14 and 21 days of culture, three sponges each were harvested and homogenized in glycine lysis buffer containing 0.1 M glycine (pH 10.4), 1 mM  $\text{MgCl}_2$  and 0.2% (v/v) TritonX-100. Each sample was centrifuged at 12,000 rpm for 5 min, and supernatant was transferred to a new centrifuge tube. The total DNA content was measured with a multiplate reader (GENius; TECAN, Männedorf, Switzerland) using the Hoechst 33258 dye method. Briefly, 100  $\mu\text{l}$  of diluted sample was mixed with 100  $\mu\text{l}$  of Hoechst 33258 in a 96-well microplate. The plate was read at 360 nm excitation and 458 nm emission. Serial dilutions of calf thymus DNA were used for preparing a standard curve.

### 2.5 Bone-associated gene expression analysis

The supplies described in this section were purchased from Invitrogen unless otherwise indicated.

Gene expressions of alkaline phosphatase (AlkP), an early-stage marker, and osteocalcin (OCN), a latter-stage marker, were measured as indicators of osteogenic activity. Glyceraldehyde-3-phosphate dehydrogenase (GAPDH) was chosen as an internal standard housekeeping gene. After 7, 10, 14 and 21 days of culture, total cellular RNA was

extracted using the TRIZOL<sup>®</sup> isolation system according to the manufacturer's instructions. One microgram of each RNA sample was used to synthesize cDNA by reverse transcription. The reverse transcription was performed at 42°C for 75 min in a reaction volume of 20  $\mu\text{l}$  containing the following: 5  $\times$  first-strand buffer, 0.1 M DTT, 2.5 mM dNTPs, random hexamer (Applied Biosystems, Foster City, CA, USA), superscript II (Applied Biosystems) and RNA solution. The reverse transcriptase in the sample was inactivated by heating at 70°C for 10 min. A polymerase chain reaction (PCR) was applied for cDNA obtained by reverse transcription to confirm gene expressions. Primers for GAPDH, AlkP and OCN were designed based on published mRNA sequences from GenBank using Primer Express software (Applied Biosystems) and were synthesized by Hokkaido System Science (Hokkaido, Japan). Table 1 shows the oligonucleotides used as PCR primers. Samples were denatured for 3 min at 94°C, followed by 30 cycles of 94°C (30 sec for GAPDH and 1 min for AlkP and OCN), annealed (55°C for 30 sec for GAPDH, 55°C for 1 min for AlkP, and 60°C for 1 min for OCN) and extended at 72°C for 1 min. This was followed by final extension at 72°C for 10 min to complete the reaction. All RT-PCR products were visualized on 1.5% (w/v) agarose gel with 0.5  $\mu\text{g}/\text{ml}$  ethidium bromide. Photographs were taken under ultra violet illumination. Real-time quantitative PCR was performed to examine the relative quantification of gene expression using ABI Prism 7000 Sequence Detection System (Applied Biosystems). cDNA was added per 25  $\mu\text{l}$  reaction with qPCR<sup>™</sup> Master Mix (EUROGENTEC Bel, Ougree, Belgium), sequence-specific primers (10  $\mu\text{M}$ ) and Taqman<sup>®</sup> MGB probes (5  $\mu\text{M}$ ). Sequences for all target gene primers and probes are shown in Table 2. Thermocycling conditions were 48°C for 30 min (reverse transcription) and 95°C for 10 min (initial denaturation) followed by 40 cycles at 95°C for 15 sec (denaturation) and 60°C for 45 sec (annealing and extension). Gene expression values were calculated based on the comparative  $\Delta\Delta\text{CT}$  method according to the description in Applied Biosystems User Bulletin Number 2 [27].

**Table 1** Alkaline phosphatase (AlkP), osteocalcin (OCN) and glyceraldehyde-3-phosphate dehydrogenase (GAPDH) primers used for the PCR analysis

Gene	Primers sequence
AlkP	F: 5'-ACCCCAAAGCCTTCTTCTTG-3' R: 5'-CGCCTGGTAGTTGTTGTGAGC-3'
OCN	F: 5'-ATGAGAGCCCTCACACTCCTC-3 R: 5'GCCGTAGAAGCGCGCCGATAGGC-3'
GAPDH	F: 5'ACCACAGTCCATGCCATCAC-3' R: TCCACCACCCTGTTGCTGTA-3'

**Table 2** Sequences for target gene primers and probes used for real-time PCR analysis

Gene	Accession number	Forward primer	Reverse primer	Taqman <sup>®</sup> MGB probe
Alkp	BCO21289	5'-atggggaaggtgaagtcg-3'	5'-taaaagcagaaatggtgacc-3'	5'-FAM-cgccaatacaccgcaatccgttgac-MGB-3'
OCN	NM_1991731	5'-caatccggactgtgacgagtt-3'	5'-ccgtagaagcgccgatagg-3'	5'-FAM-cacatcgctttcag-MGB-3'
GAPDH	NM_002046	5'-atggggaaggtgaagtcg-3'	5'-taaaagcagaaatggtgacc-3'	5'-FAM-cgccaatacaccgcaatccgttgac-MGB-3'

2.6 Statistical analysis

The in vitro cellular tests were performed in triplicate (proliferation and gene expression) for each condition, and the data were represented as mean ± SD. Statistical difference was analyzed using one-way analysis of variance (ANOVA), and *P* values less than 0.05 were considered significant.

3 Results

3.1 Characterization of HAp/Col nanocomposite sponge

The mass ratio of HAp in the HAp/Col nanocomposite calculated from the TG-DTA data was  $69.53 \pm 0.57\%$  (w/w), as expected (70%) from the starting materials ratio. Porous HAp/Col composite sponges were successfully prepared as shown in Fig. 3, even without adding collagen suspension on preparation. The mean porosity was calculated to be  $94.8 \pm 0.4\%$  from the weight and volume. Wet HAp/Col sponges demonstrated sponge-like, viscoelastic behavior against compression as shown in Fig. 3 as previously reported [20]. Figure 4 shows a surface SEM image of the HAp/Col sponge, which seemed to be rougher than that of the conventional culture plate and excellent for cell attachment. However, the pore size was  $248.3 \pm 89.3 \mu\text{m}$  (range: 88–508  $\mu\text{m}$ ), which was 4.65 times greater than that of Col sponge,  $53.4 \pm 20.7 \mu\text{m}$  (range: 27–144  $\mu\text{m}$ ). The wall thickness,  $71.3 \pm 44.2 \mu\text{m}$  (range: 18–202  $\mu\text{m}$ ) of the

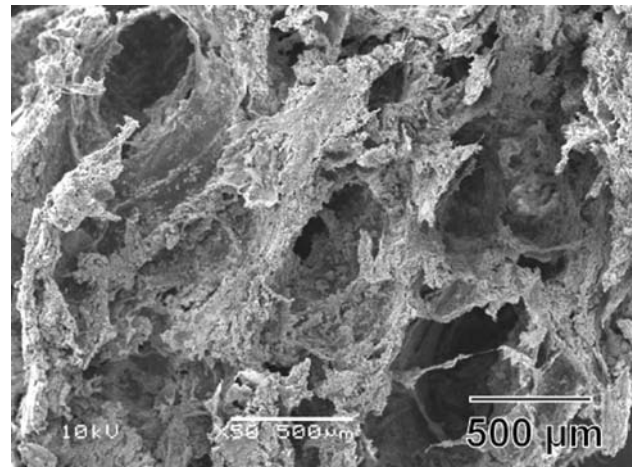


**Fig. 4** A surface SEM image of the HAp/Col sponge

HAp/Col sponge were greater than those of the Col sponge,  $6.50 \pm 2.65 \mu\text{m}$  (range: 2.3–12.8  $\mu\text{m}$ ).

3.2 Histological findings

MG63 cells seeded onto the HAp/Col sponges attached to the pore surface and continued to grow into the sponges in vitro. At 1 day after cell seeding (Day 1), the cells demonstrated good initial attachment to the surfaces of both sponges as shown in SEM micrographs (Fig. 5a, b). According to the SEM observations at Day 7, cells showed good migration and proliferation into the HAp/Col sponge as well as on the surface of the sponge (Fig. 5c). Most of the

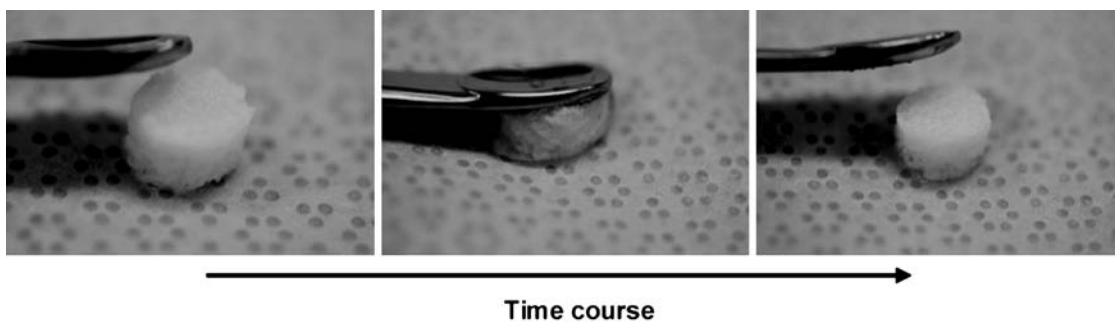
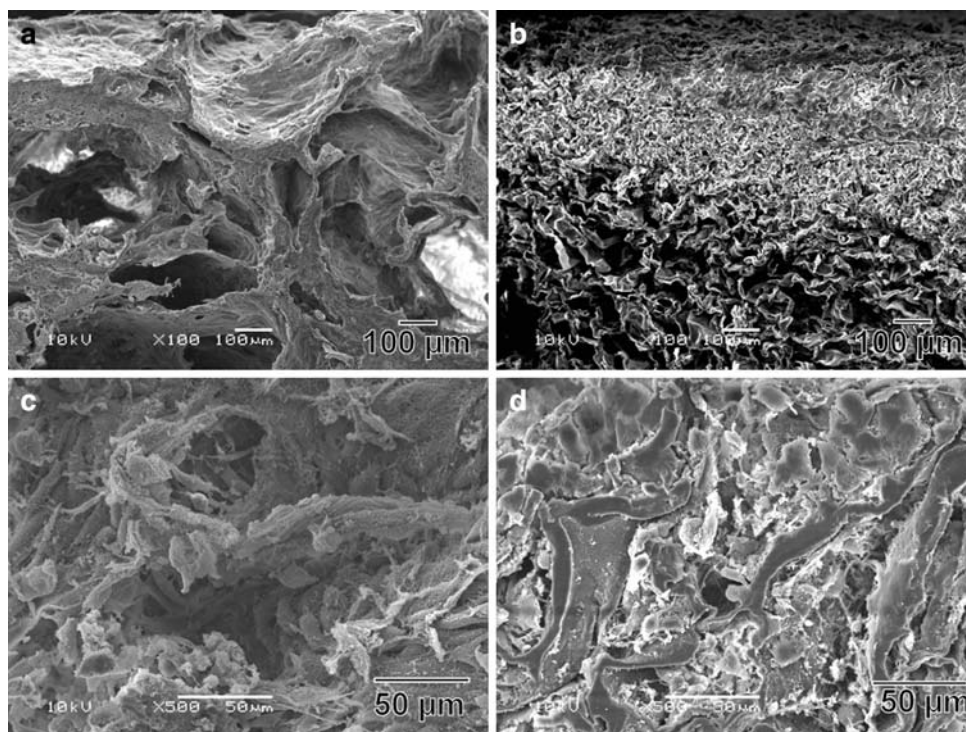


**Fig. 3** Sponge-like, viscoelastic property of a wet HAp/Col sponge against compression

**Fig. 5** SEM images of the HAp/Col sponge (a) and on the Col sponge (b) at 1 day after cell seeding and the HAp/Col sponge (c) and Col sponge (d) at 7 days



cells were filling the external layer of the Col sponge approximately 500  $\mu\text{m}$  in depth (Fig. 5d); however, a few cells were observed also in the inner region. At Day 21, the cells proliferated to cover the surface of both sponges completely and grew outward (Fig. 6a, b). The cells also proliferated in the inner region, even at the centers, of the HAp/Col sponge (Fig. 6c). In contrast, only a few cells were observed in the inner region of the Col sponge (Fig. 6d). No pyknotic cells were observed in the center of both sponges. Scanning electron micrographs (Fig. 6e, f) also showed that the cells were well attached to the walls of both sponges and formed extracellular matrices (ECMs) around them. Furthermore, deposition of calcium phosphate, which was assumed to be HAp due to stability in the biological environment, was confirmed on both cells and ECMs in the HAp/Col sponge by the SEM and EDS point analyses (Fig. 7), but it was not observed in the Col sponge.

### 3.3 Total DNA content

The total DNA content analysis demonstrated that the cell number in the HAp/Col sponge was smaller than that in the Col sponge at early stages of the culture as shown in Fig. 8. However, the HAp/Col sponge resulted in greater overall proliferation compared to the Col sponge; the total DNA contents at Day 14 and 21 in the HAp/Col sponge were significantly higher than those in the Col sponge. At Day 21, total DNA content in the HAp/Col sponge was approximately 1.8 times greater than that in the Col sponge.

### 3.4 Gene expression

The results of the conventional RT-PCR analysis to assess the expression of bone-associated gene are shown in Fig. 9. All samples showed good expression of housekeeping gene, GAPDH. The bone-associated genes showed a different trend. Strong AlkP expression was observed in all of the samples, while OCN gene expression was barely detected at Day 7 in both sponges. The relative amount of OCN expression was increased at Day 10 and gradually decreased until Day 21. The real-time quantitative RT-PCR analysis showed that AlkP gene expression in the HAp/Col sponge was increased with time as shown in Fig. 10a. On the contrary, AlkP expression in the Col sponge remained at similar levels. As a result, although AlkP gene expression in the HAp/Col sponge was significantly smaller than that in the Col sponge at Day 7 and 10, it showed greater trend at Day 21 (no significant difference). As shown in Fig. 10b, OCN gene expression, the latter-stage marker of osteogenic activity, showed no significant difference between the HAp/Col and Col group but trend of earlier expression in the HAp/Col sponge than in the Col sponge.

## 4 Discussion

The ability of biomaterial scaffolds to support migration of cells from surrounding tissues is a key parameter in tissue engineering. Three-dimensional porous scaffolds may

**Fig. 6** Histological sections stained with hematoxylin and eosin, and SEM images at Day 21. The cells proliferated to cover the surface of the HAp/Col sponge (a) and that of the Col sponge (b). The cells also proliferated into the center part of the HAp/Col sponge (c), but only a few cells were observed in the inner region of the Col sponge (d). By SEM, cells were well attached to the walls of the HAp/Col sponge (e) and the Col matrices (f) forming extracellular matrices (ECMs)

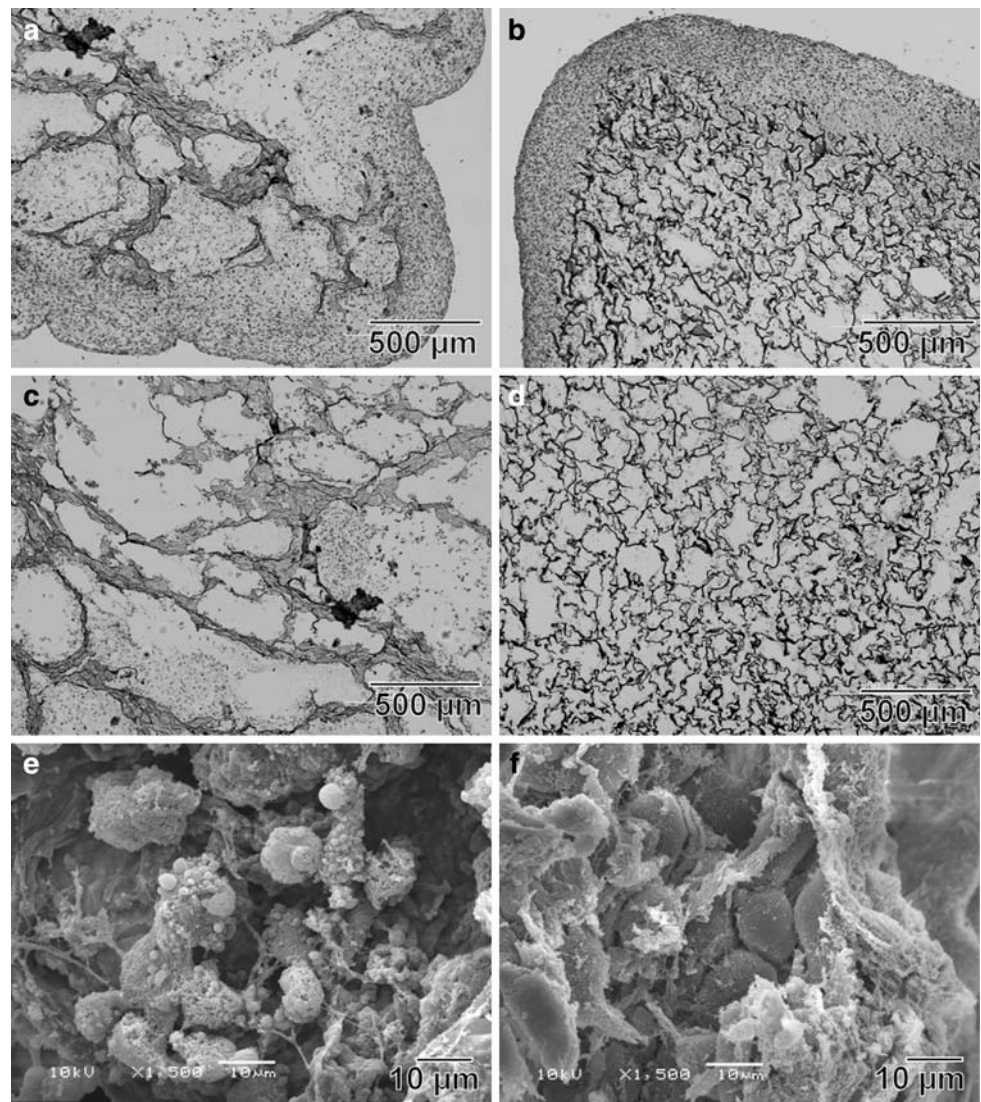
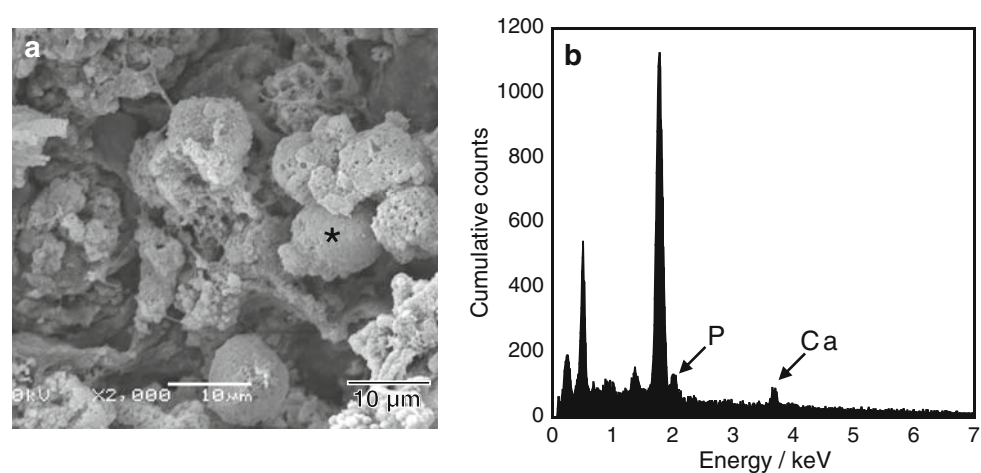


**Fig. 7** SEM and EDS point analyses of the HAp/Col sponge at Day 21. Calcium phosphate was deposited on both cells and ECMs. The asterisk indicates the point of EDS analysis



enhance bone regeneration by creating and maintaining a space that facilitates progenitor cell migration, proliferation and differentiation. Culture of osteoblast-like cells

seeded in 3D biocompatible and osteoconductive scaffolds in vitro is a promising approach to produce an osteoinductive material for the repair of bone defects. Bone is a

composite material made up of collagen protein fibers threading through a HAp mineral phase, which makes up about 70% of the bone structure [28]. The HAp and Col

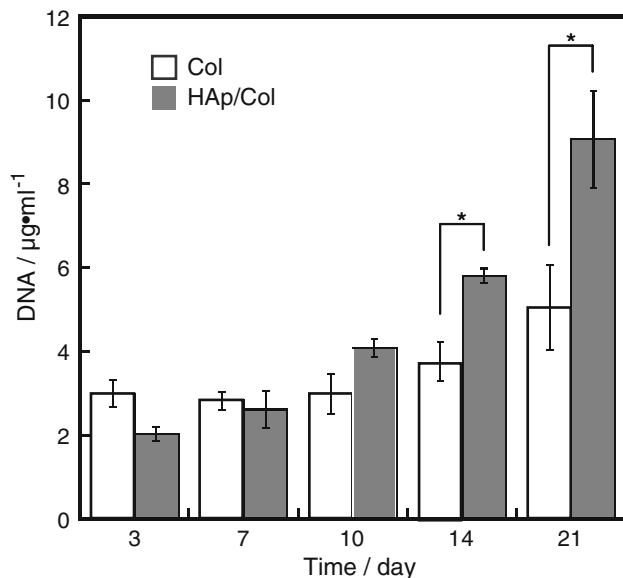


**Fig. 8** Total DNA content from the two sponges. Asterisks indicate the statistical significances between the two examinations ( $P < 0.05$ )

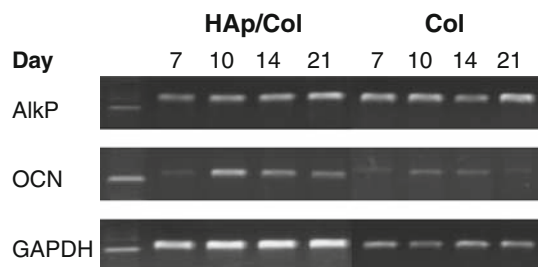
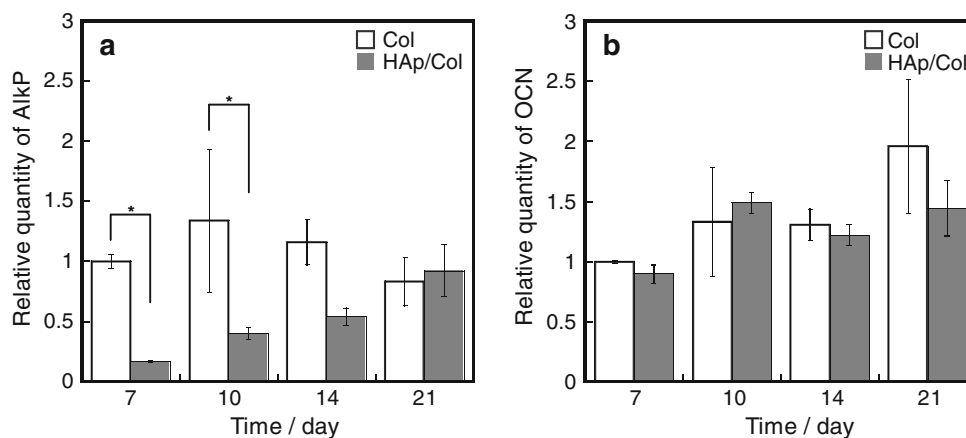


**Fig. 9** Conventional RT-PCR analysis to assess expression of bone-associated genes in both sponges. AlkP, alkaline phosphatase; OCN, osteocalcin; GAPDH, glyceraldehyde-3-phosphate dehydrogenase

**Fig. 10** Real-time quantitative RT-PCR analysis to quantify alkaline phosphatase (a) and osteocalcin gene expressions in the two sponges. Asterisks indicate the statistical significances between the two examinations ( $P < 0.05$ )



mass ratio in the HAp/Col sponge prepared was 68.99/31.01, which was almost identical to the theoretical value calculated from the amounts of the starting materials, i.e., 70/30. This preparation method can successfully precipitate HAp/Col nanocomposite while maintaining the starting material ratio. A scaffold for tissue engineering should possess a 3D porous structure with porosity no less than 70% (v/v) and pore size ranging from 50 to 900  $\mu\text{m}$  [29, 30], because the degree of porosity and the diameter of pores always influence the mechanical property of the scaffold. We prepared a highly porous HAp/Col nanocomposite sponge that has sponge-like, viscoelastic properties under wet conditions. The HAp/Col sponge is expected as a favorable bone filler and tissue engineering scaffold material for this mechanical property, because viscoelasticity allows the sponge to deform and fit into the bone defect of any shape or even into a defect smaller than the sponge dimension. The viscoelastic property also allows cutting of the material in appropriate shapes and sizes with scissors, a surgical knife or even by hand tearing. Finally, the property inhibits unexpected breakage of the material and formation of debris from the surface during surgical operation. From the SEM observation of the HAp/Col sponge, pores were mainly composed of macropores ranging 100–500  $\mu\text{m}$  in diameter. The pore size was appropriate for mineralized bone formation in the sponge [31]. If the appropriate pore size and interconnection were guaranteed as the present study, the more open-spaced the scaffold is, the larger the space and surface area for cell migration and proliferation. Good cell attachment in the initial stage, appropriate spaces for cell proliferation and migration, and an appropriately interconnected porous structure for tissue formation are necessary for the tissue engineering scaffold. MG63 cells attached to the HAp/Col sponge surface as well as the Col sponge from the initial stage of the experiment. Furthermore, significantly better cellular migration and proliferation were observed with the



HAp/Col sponge than those with the Col sponge in the latter stage of the experiment, because the pore and interconnected pathway sizes of the HAp/Col sponge were greater than those of the Col sponge. Accordingly, few cells on the Col sponge could migrate into the inner layer.

DNA content and AlkP gene expression were smaller in the cells in the HAp/Col sponge than that in the Col sponge in the early stage because of the difference in cell densities. Generally, cell proliferation and AlkP gene expression of osteoblast-like cells are influenced by cell–cell interaction, i.e., usually equivalent with cell density. For example, Interpore<sup>®</sup> is a highly interconnected and porous HAp prepared from coral which confirmed good bone formation ability *in vivo*; however, Matsuhima et al., reported that cells cultured on Interpore<sup>®</sup> need a longer time to express high activity of AlkP *in vitro* in comparison to the cells cultured on other porous HAp [32]. The reason why was that cell migration on Interpore<sup>®</sup> could be too good to reach enough cell density to activate high AlkP gene expression in the early stage. In the present result, the peripheral layer of the Col sponge was filled with cells and formed cell–cell interaction even in the early stages. On the contrary, cells on the HAp/Col sponge migrated into the inside and did not form obvious cell–cell interaction in the early stages. OCN gene expression showed a tendency to increase in the HAp/Col sponge at early stages, although in the Col sponge it increased at later stages. This may indicate that osteogenic activity increases earlier in the HAp/Col sponge even without high AlkP activity in comparison to the Col sponge. Since bone formation is a complex sequence of events that begins with the recruitment and proliferation of osteoprogenitor cells followed by cellular differentiation, osteoid formation and ultimately mineralization [33]. We used MG63 cells to examine their osteogenic activity in the HAp/Col sponge for a bone tissue engineering scaffold. The results indicated that MG63 cells became securely attached to the material surfaces, maintaining good proliferation and showing good osteogenic gene expressions in the HAp/Col sponge. Finally, calcium phosphate was deposited on the ECMs in the HAp/Col sponge at a latter stage, i.e., bone-like substance was formed *in vitro* in the HAp/Col sponge. The histological and SEM observations, EDS analysis and total DNA amount measurement proved that MG63 cells were well attached to and proliferated within the HAp/Col sponge, and that calcification occurred during the culture period. Concerning the present results, we are planning to evaluate the HAp/Col sponge by primary cell culture to prove its usefulness for bone tissue engineering scaffold to repair extremely large bone defect.

## 5 Conclusions

In this study, adhesion, proliferation and osteogenic responses of MG63 cells in the 3D highly porous HAp/Col sponge were investigated under the pressure/perfusion culture. The HAp/Col sponge prepared without adding supplemental collagen suspension demonstrated sponge-like, viscoelastic behavior under wet condition as well as the HAp/Col sponge prepared with adding supplemental collagen suspension described in ref. 20. The MG63 cells attached very well on the HAp/Col sponge as the same as that on the Col sponge; however, cell migration and proliferation in the HAp/Col sponge, especially in the later stage, were quite better than those in the Col sponge. The cells were viable even at the center of both sponges under pressure/perfusion culture. Total DNA content in the HAp/Col sponge at Day 21 was 1.8 times greater than that in the Col sponge. MG63 cells showed good osteogenic gene expressions in the HAp/Col sponge as well as in the Col sponge. Furthermore, calcification on the cell surfaces and in ECMs was observed by SEM with the HAp/Col sponge at Day 21, but not with the Col sponge. The HAp/Col sponge is a good candidate bone tissue engineering scaffold due to its sponge-like visco-elasticity, its microstructure for cell migration and enhancement of osteogenic activity including calcification of the ECM.

## References

1. Cornell CN, Lane JM. Current understanding of osteoconduction in bone regeneration. *Clin Orthop Relat Res.* 1998;355:S267–73.
2. Mikos AG, Thorsen AJ, Czerwonka LA, Bao Y, Langer R, Winslow DN, et al. Preparation and characterization of poly (L-lactic acid) foams. *Polymer.* 1994;35:1068–77.
3. Quirk RA, Davies MC, Tendler SJB, Shakesheff KM. Surface engineering of poly (lactic acid) by entrapment of modifying species. *Macromolecules.* 2000;33:158–260.
4. Ma PX, Langer R. Degradation, structure and properties of fibrous nonwoven poly(glycolic acid) scaffolds for tissue engineering. In: Mikos AG, et al., editors. *Polymers in medicine and pharmacy.* Pittsburgh: MRS; 1995. p. 99–104.
5. Shea LD, Wang D, Franceschi RT, Mooney DJ. Engineered bone development from a pre-osteoblast cell line on three-dimensional scaffolds. *Tissue Eng.* 2000;6:605–17.
6. Goldstein AS, Zhu G, Morris GE, Meszlenyi RK, Mikos AG. Effect of osteoblastic culture conditions on the structure of poly (DL-lactic-co-glycolic acid) foam scaffolds. *Tissue Eng.* 1999;5: 421–34.
7. Ishaug-Riley SL, Crane-Kruger GM, Yaszemski MJ, Mikos AG. Three-dimensional culture of rat calvarial osteoblasts in porous biodegradable polymers. *Biomaterials.* 1998;19:1405–12.
8. Goldstein AS, Juarez TM, Helmke CD, Gustin MC, Mikos AG. Effect of convection on osteoblastic cell growth and function in biodegradable polymer foam scaffolds. *Biomaterials.* 2001; 22:1279–88.

9. Ishaug SL, Crane GM, Miller MJ, Yasko AW, Yaszemski MJ, Mikos AG. Bone formation by three-dimensional stromal osteoblast culture in biodegradable polymer scaffolds. *J Biomed Mater Res.* 1997;36:17–28.
10. Wang H, Li Y, Zuo Y, Li L, Ma S, Cheng L. Biocompatibility and osteogenesis of biomimetic nano-hydroxyapatite/polyamide composite scaffolds for bone tissue engineering. *Biomaterials.* 2007;28:3338–48.
11. Shor L, Güçeri S, Wen X, Gandhi M, Sun W. Fabrication of three-dimensional polycaprolactone/hydroxyapatite tissue scaffolds and osteoblast-scaffold interactions in vitro. *Biomaterials.* 2007;28:5291–7.
12. Ignjatović N, Tomić S, Dakić M, Miljković M, Plavsić M, Uskoković D. Synthesis and properties of hydroxyapatite/poly-L-lactide composite biomaterials. *Biomaterials.* 1999;20:809–16.
13. Vert M, Mauduit J, Li S. Biodegradation of PLA/GA polymers: increasing complexity. *Biomaterials.* 1994;15:1209–13.
14. Rovira A, Amedee J, Bareilleand R, Rabaud M. Colonization of a calcium phosphate/elasticin-solubilized peptide-collagen composite material by human osteoblasts. *Biomaterials.* 1996;17:1535–40.
15. Wang X, Grogan SP, Rieser F, Winkelmann V, Maquet V, Berge ML, et al. Tissue engineering of biphasic cartilage constructs using various biodegradable scaffolds: an in vitro study. *Biomaterials.* 2004;25:3681–8.
16. Du C, Cui FZ, Zhu XD, de Groot K. Three-dimensional nano-HAp/collagen matrix loading with osteogenic cells in organ culture. *J Biomed Mater Res.* 1999;44:407–15.
17. Wu TJ, Huang HH, Lan CW, Lin CH, Hsu FY, Wang YJ. Studies on the microspheres comprised of reconstituted collagen and hydroxyapatite. *Biomaterials.* 2004;25:651–8.
18. Clarke KI, Graves SE, Wong ATC, Triffitt JT, Francis MJO, Czernuszka JT. Investigation into the formation and mechanical properties of a bioactive material based on collagen and calcium phosphate. *J Mater Sci Mater Med.* 1993;4:107–10.
19. Kikuchi M, Itoh S, Ichinose S, Shinomiya K, Tanaka J. Self-organization mechanism in a bone-like hydroxyapatite/collagen nanocomposite synthesized in vitro and its biological reaction in vivo. *Biomaterials.* 2001;22:1705–11.
20. Kikuchi M, Ikoma T, Syoji D, Matsumoto HN, Koyama Y, Itoh S, et al. Porous body preparation of hydroxyapatite/collagen nanocomposites for bone tissue regeneration. *Key Eng Mater.* 2004;254:561–4.
21. Cartmell SH, Porter BD, Garcia AJ, Guldberg RE. Effect of medium perfusion rate on cell-seeded three-dimensional bone constructs in vitro. *Tissue Eng.* 2003;9(6):1197–203.
22. Glowacki J, Mizuno S, Greenberger JS: perfusion enhances functions of bone marrow stromal cells in three-dimensional culture. *Cell Transplant.* 1998;7(3):319–26.
23. Muller SM, Mizuno S, Gerstendfeld LC, Glowacki J. Medium perfusion enhances osteogenesis by murine osteosarcoma cells in three-dimensional collagen sponge. *J Bone Min Res.* 1999;14: 2118–26.
24. Mizuno S, Tateishi T, Ushida T, Glowacki J. Hydrostatic fluid pressure enhances matrix synthesis and accumulation by bovine chondrocytes in three-dimensional culture. *J Cell Phys.* 2002; 193:319–27.
25. Kikuchi M, Kikuchi K, Johnson K, Glowacki J. Hydrostatic fluid pressure stimulates osteogenesis by MG63 cells in porous collagen sponge. *J Oromaxillo facial Biomech.* 2004;10(1):57–60.
26. Meinel L, Karageorgiou V, Fajardo R, Snyder B, Shinde-Patil V, Zichner L, et al. Bone tissue engineering using human mesenchymal stem cells: effects of scaffold material and medium flow. *Ann Biomed Eng.* 2004;32(1):112–22.
27. Applied Biosystems (2001) Applied biosystems user bulletin number 2, Foster City, CA [Kikuchi M, Kikuchi K, Johnson K, Glowacki J. Hydrostatic fluid pressure stimulates osteogenesis by MG63 cells in porous collagen sponge. *J Oromaxillo Facial Biomech* 2004;10(1):57–60] Ritter SK. *Boning up.* *Chem Eng News* 1997;75:27–32.
28. Salgado AJ, Coutinho OP, Reis RL. Bone tissue engineering: state of the art and future trends. *Macromol Biosci.* 2004;4:743–65.
29. Hutmacher DW. Scaffolds in tissue engineering bone and cartilage. *Biomaterials.* 2000;21:2529–43.
30. Ma PX. Scaffolds for tissue fabrication. *Mater Today.* 2004;7(5): 30–40.
31. Cerroni L, Filocamo R, Fabbri M, Piconi C, Caropreso S, Condo SG. Growth of osteoblast-like cells on porous hydroxyapatite ceramics: an in vitro study. *Biomol Eng.* 2002;19(2–6):119–24.
32. Matsushima A, Kotobuki N, Tadokoro M, Ohgushi H. Comparative study of ceramics structure for culturing human mesenchymal stromal cells. *Key Eng Mater.* 2008;361–3:1067–70.
33. Yang XB, Roach HI, Clarke NMP, Howdle SM, Quirk R, Shakesheff KM, et al. Human osteoprogenitor growth and differentiation on synthetic biodegradable structures after surface modification. *Bone.* 2001;29:523–31.